Mathematical Determination of Stresses and Displacements in Star-Perforated Grains

HOWARD B. WILSON JR.*
University of Alabama, University, Ala.

A mathematical method is presented for determining stresses in solid propellant rocket grains due to pressurization, steady thermal gradients, and uniform propellant shrinkage. The type of solid propellant grain considered is a long cylinder containing a longitudinal perforation with an arbitrary number of identical star points of general shape. The external boundary of the propellant grain is bonded to a circular-cylindrical motor case. The propellant has constant mechanical and thermal properties and is in a state of plane strain. Linear elasticity theory and complex variable methods are used to formulate a general stress problem for a doubly connected region that has a star-shaped internal boundary and a circular external boundary and is subjected to steady thermal gradients and uniform boundary pressures. This problem is solved approximately by considering a related problem for an infinite plane with a star-shaped hole. Effects of bonding the external boundary to an elastic case are deduced approximately by superposition. A general stress program for a digital computer is described, and example computations testing the validity of the assumed approximations are made. The method is found to provide a practical means of analyzing stresses in solid propellant grains.

Introduction

THE analysis of stress concentrations in the propellant grain of a solid propellant rocket motor under various loading conditions is of considerable importance. Geometrical complexities and time and temperature varying physical properties of the material make exact determination of these stresses very difficult. In analyzing such problems, either mathematically or experimentally, simplifying assumptions must be made which reduce the problem complexity but still yield practical results.

This paper considers the determination of stresses due to pressurization, steady thermal gradients, and propellant shrinkage in case-bonded grains. It is assumed that the propellant is in a state of plane strain, is linearly elastic, and has constant thermal and mechanical properties. The solution presented is well suited for digital computer coding and complete FORTRAN programs for the IBM 7090 have been written.[1, 2] The methods developed can be readily extended to include viscoelastic material properties.[3]

The type of motor considered has a long cylindrical case filled with a solid propellant which is bonded to the case and contains a perforation along the longitudinal axis of the case. The geometrical configuration of the propellant cross section has a circular external boundary and an internal boundary consisting of an arbitrary number of identical and symmetrical star points of general shape. The shape and number of the star points depend on the required thrust program for the motor.

The assumed boundary loading consists of uniform pressure at the internal boundary of the grain with the external boundary being either bonded to the motor case or uniformly pressurized. Steady thermal stresses due to different constant internal and external temperatures are also determined, with propellant shrinkage effects being included as a particular instance of the thermal stress problem.

Extensive photoelastic investigations on elastic media have been made to evaluate propellant grain stress concentrations due to pressurization and uniform temperature change.[4–6] A mathematical study of stresses due to internal pressure in a grain with four star points was also made previously by this author,[7] and close agreement between the theoretical and photoelastic results was shown in Ref. 6. The present paper significantly extends and generalizes Ref. 7 to account for arbitrary grain geometry, temperature and shrinkage effects, and effects of pressurization.

The analysis employs complex function theory and is based on determination of two functions analytic in an annulus and satisfying two boundary-value equations related to stress conditions on the internal and external boundaries of the propellant grain. It is shown that, by considering a related stress problem for an infinite plane with a star-shaped hole, the stress conditions for the internal boundary of the grain can be exactly satisfied, with the external boundary conditions being satisfied except for small residual stresses that have a negligible influence near the internal boundary where accurate stress determination is most important. The effect of bonding the external boundary of the grain to an elastic case is determined by a superposition procedure similar to that developed in Ref. 7.

Example computations are presented for thermal stresses in a typical six-pointed grain configuration having zero applied boundary loading. It is found that the approximate method for satisfying the boundary conditions yields good results unless the web fraction† is small.

Although determination of stresses in star-perforated propellant grains is of principal interest here, it should be mentioned that the solution is obtained in terms of a general mapping function pertaining to a doubly connected region with a circular external boundary and an internal boundary consisting of an arbitrary number of identical and symmetrical parts. In addition to star-shaped configurations, this geometry also includes other common shapes such as rectangles and equilateral triangles with straight or arbi-

Received October 2, 1963; revision received April 22, 1964. The results contained in this paper were taken from the author's Ph.D. Dissertation in Theoretical and Applied Mechanics, University of Illinois, January 1963. The investigation was sponsored by Rohm & Haas Company, Huntsville, Ala., under U.S. Army Contract DA-01-021-ORD-11878.

* Associate Professor of Engineering Mechanics and Applied Mathematics, University of Alabama; also Consultant to Rohm & Haas Company. Member AIAA.

† The web fraction is defined as the grain thickness along the star-point bisector divided by the radius of the outer boundary.

trarily rounded corners. Thus, one could treat by exactly the same method, for instance, stress problems for a circular cylinder containing a square hole.

Complex Variable Formulation of the Stress Problem

It will be assumed that an annulus in the ζ plane can be mapped onto the stressed doubly connected region in the z plane by a function of the general form

$$z = \omega(\zeta) = \sum_{n=0}^{n=m} C_n \zeta^{1-np} \qquad 1 \leq |\zeta| \leq b \qquad (1)$$

where m is an arbitrary integer, the C_n are real constants, and p is the number of symmetry axes of the geometry.[8] The required mapping function will be considered known. An accurate general method for determining the mapping function for a geometry of this type is developed in Refs. 1 and 2. The mapping correspondence defined by $\omega(\zeta)$ is illustrated in Fig. 1 by an example from Ref. 1 for $p = 6$ and $m = 49$. This same configuration is employed in the example stress computations presented below.

The mapping function defined by Eq. (1) transforms the circle $|\zeta| = b$ into a contour that deviates slightly from a circle, but this deviation is insignificant in most instances. A measure of the deviation is given by the ratio

$$f = [\omega(b) - |\omega(be^{i\pi/p})|]/\omega(b)$$

Typically, for the geometry in Fig. 1 and web fractions of 19 and 50%, the values of f were found to be 0.0106 and 0.003, respectively. It will be assumed below that, for all practical purposes, $|\zeta| = b$ maps into a circle.

The stressed region will be designated as R with the applied uniform internal and external boundary pressures being P_0 and P_1, respectively. The internal and external temperatures will be similarly denoted by U_0 and U_1. The region will be assumed unstressed for zero boundary pressures and zero reference temperature. The condition of uniform external pressure will be modified later by superposition to account for an elastic case.

Under the transformation given by Eq. (1), the system of circles and radial lines about the origin of the ζ plane maps into an orthogonal curvilinear coordinate system in the z plane. It is well known that, in the absence of thermal effects, the stresses and displacements relative to the curvilinear coordinate system in R can be determined in terms of two complex stress functions $\varphi_1(\zeta)$ and $\psi_1(\zeta)$. Furthermore, problems involving steady thermal gradients can be reduced to associated problems with thermal effects excluded and modified boundary conditions.[9] In the absence of thermal effects, the stresses and displacements relative to the curvilinear coordinate system are given by

$$\sigma_\rho + \sigma_\theta = 2\left[\frac{\varphi_1'(\zeta)}{\omega'(\zeta)} + \overline{\frac{\varphi_1'(\zeta)}{\omega'(\zeta)}}\right] \qquad (2)$$

$$-\sigma_\rho + \sigma_\theta + 2i\sigma_{\rho\theta} = \frac{2\zeta^2}{\rho^2\overline{\omega'(\zeta)}}\left[\overline{\omega(\zeta)}\,\frac{d}{d\zeta}\left(\frac{\varphi_1'(\zeta)}{\omega'(\zeta)}\right) + \psi_1'(\zeta)\right] \qquad (3)$$

and

$$2\mu(u_\rho + iu_\theta) = \frac{\bar{\zeta}\,\overline{\omega'(\zeta)}}{\rho|\omega'(\zeta)|}\left[\kappa\varphi_1(\zeta) - \frac{\omega(\zeta)\overline{\varphi_1'(\zeta)}}{\overline{\omega'(\zeta)}} - \overline{\psi_1(\zeta)}\right] \qquad (4)$$

where σ_ρ, σ_θ, and $\sigma_{\rho\theta}$ are the curvilinear stress components, u_ρ and u_θ are curvilinear displacement components, μ is the shear modulus, and $\kappa = 3 - 4\nu$ for plane strain, with ν being Poisson's ratio.

The boundary conditions on R can be expressed in the form

$$\varphi_1(t) + \frac{\omega(t)\overline{\varphi_1'(t)}}{\overline{\omega'(t)}} + \overline{\psi_1(t)} = \int (N + iT)\omega'(t)dt + k_j \qquad (5)$$

where t denotes the complex variable on either boundary of the annulus $1 \leq |\zeta| \leq b$, N and T are boundary normal and shear stresses, and k_j are constants generally different for each boundary of R. In the problem considered here, the k_j can be taken equal to zero.

Plane problems involving steady thermal stresses can be reduced to associated problems excluding thermal effects[9] by taking the Cartesian displacement components in the form

$$u^T + iv^T = u_1 + iv_1 + u^* + iv^* \qquad (6)$$

where $u^T + iv^T$ denotes the total displacement due to the combined effect of thermal gradients and boundary loading, $u_1 + iv_1$ denotes a modified displacement function, and $u^* + iv^*$ denotes an effective thermal displacement function corresponding to zero stresses and is defined by

$$u^* + iv^* = (1 + \nu)\alpha \int G(z)dz \qquad (7)$$

with α being the coefficient of thermal expansion and $G(z)$ an analytic function with its real part equal to the steady temperature distribution in the region of interest. It is evident that, for a given temperature field, $G(z)$ will be determined within the limits of a pure imaginary constant. Furthermore, changing $G(z)$ by an imaginary constant and adding an arbitrary complex constant to the right side of Eq. (7) only changes $u^* + iv^*$ by an insignificant rigid body displacement. Thus, problems involving steady thermal gradients can be reduced to associated problems involving the actual stress components and the modified displacements $u_1 + iv_1$. The associated problem can be solved by complex variable methods.

The steady temperature field in R, because of constant internal and external temperatures U_0 and U_1, can be written as a function of ζ as

$$U(\zeta) = Re\left[U_0 + \frac{(U_1 - U_0)}{\ln(b)}\ln(\zeta)\right] \qquad (8)$$

It then follows that, when Eq. (7) is expressed in terms of ζ by means of the mapping function, use of Eq. (8) yields

$$u^* + iv^* = (1 + \nu)\alpha U_0\omega(\zeta) + \frac{(1 + \nu)\alpha(U_1 - U_0)}{\ln(b)}\omega(\zeta)\ln(\zeta) - \frac{(1 + \nu)\alpha(U_1 - U_0)}{\ln(b)}\sum_{n=0}^{n=m} C_n(1 - np)^{-1}\zeta^{1-np} \qquad 1 \leq |\zeta| \leq b \qquad (9)$$

Because of the term $\omega(\zeta)\ln(\zeta)$ in Eq. (9), $u^* + iv^*$ is a multivalued function.

The solution of the stress problem can now be reduced to determining two stress functions $\varphi_1(\zeta)$ and $\psi_1(\zeta)$, which are analytic for $1 \leq |\zeta| \leq b$, give normal stresses of $-P_0$ and $-P_1$ for $|\zeta| = 1$ and $|\zeta| = b$, respectively, and give multivalued displacements $u_1 + iv_1$ which, when added to $u^* + iv^*$, yield the total displacements that must be single-valued.

For a counterclockwise circuit about $\zeta = 0$, $u^* + iv^*$ undergoes a change:

$$\Delta(u^* + iv^*) = \frac{2\pi i(1 + \nu)\alpha(U_1 - U_0)}{\ln(b)}\omega(\zeta) \qquad 1 \leq |\zeta| \leq b \qquad (10)$$

Therefore, it follows from the Cartesian form of Eq. (4) and from Eq. (6) that

$$u_1 + iv_1 = \frac{1}{2\mu}\left[\kappa\varphi_1(\zeta) - \frac{\omega(\zeta)\overline{\varphi_1'(\zeta)}}{\overline{\omega'(\zeta)}} - \overline{\psi_1(\zeta)}\right] \qquad (11)$$

must undergo a change which cancels that given by Eq. (10). The necessary multivalued behavior of $u_1 + iv_1$ can be obtained by taking $\varphi_1(\zeta)$ and $\psi_1(\zeta)$ in the form

$$\varphi_1(\zeta) = -K\omega(\zeta)\ln(\zeta) + \varphi(\zeta)$$
$$\psi_1(\zeta) = \psi(\zeta) \tag{12}$$

where $\varphi(\zeta)$ and $\psi(\zeta)$ are single-valued functions expandable in Laurent series about $\zeta = 0$. The constant K is given by

$$K = (U_1 - U_0)\alpha E/4(1-\nu)\ln(b) \tag{13}$$

Since the boundary loading consists of uniform internal and external pressures P_0 and P_1, respectively, it follows from Eq. (5) that

$$\varphi_1(\zeta_j) + \frac{\overline{\omega(\zeta_j)}\varphi_1'(\zeta_j)}{\overline{\omega'(\zeta_j)}} + \overline{\psi_1(\zeta_j)} = -P_j\omega(\zeta_j) \qquad j = 0, 1 \tag{14}$$

where $\zeta_j = \rho_j\sigma$, $\sigma = e^{i\theta}$, $\rho_0 = 1$, and $\rho_1 = b$. Then, with the use of Eqs. (12), the boundary conditions satisfied by $\varphi(\zeta)$ and $\psi(\zeta)$ are found to be

$$\varphi(\zeta_j) + \frac{\omega(\zeta_j)\overline{\varphi'(\zeta_j)}}{\overline{\omega'(\zeta_j)}} + \overline{\psi(\zeta_j)} = [2K\ln|\zeta_j| - P_j]\omega(\zeta_j) + \frac{K\omega(\zeta_j)\overline{\omega(\zeta_j)}}{\zeta_j\,\overline{\omega'(\zeta_j)}} \qquad j = 0, 1 \tag{15}$$

It is convenient to think of a stress problem pertaining to the functions $\varphi(\zeta)$ and $\psi(\zeta)$ and the boundary equations (15). It follows from Eq. (5) that the boundary stresses in this problem are given by

$$N_j + iT_j = -P_j + 2K\ln|\zeta_j| + K\frac{\overline{\omega(\zeta_j)}}{\bar{\zeta}_j\,\overline{\omega'(\zeta_j)}} - K\frac{\omega(\zeta_j)}{\zeta_j\omega'(\zeta_j)} + K\left|\frac{\omega(\zeta_j)}{\omega'(\zeta_j)}\right|^2\left[\frac{1}{|\zeta_j|^2} + \frac{\omega''(\zeta_j)}{\zeta_j\omega'(\zeta_j)}\right] = 0, 1 \tag{16}$$

Because of the symmetry of the boundary loading, $\varphi(\zeta)$ and $\psi(\zeta)$ will have the following series forms:

$$\varphi(\zeta) = \sum_{n=-\infty}^{n=\infty} a_n\zeta^{1-np} \qquad 1 \le |\zeta| \le b \tag{17}$$

and

$$\psi(\zeta) = \sum_{n=-\infty}^{n=\infty} b_n\zeta^{-1-np} \qquad 1 \le |\zeta| \le b \tag{18}$$

where the a_n and b_n are real.

When $\varphi(\zeta)$ and $\psi(\zeta)$ have been evaluated by some means, the stresses are obtained by substituting Eqs. (12) into Eqs. (2) and (3). This yields

$$\sigma_\rho{}^T + \sigma_\theta{}^T = -2K\left[\frac{\omega(\zeta)}{\zeta\omega'(\zeta)} + \frac{\overline{\omega(\zeta)}}{\bar{\zeta}\,\overline{\omega'(\zeta)}} + 2\ln(\rho)\right] + 2\left[\frac{\varphi'(\zeta)}{\omega'(\zeta)} + \frac{\overline{\varphi'(\zeta)}}{\overline{\omega'(\zeta)}}\right] \tag{19}$$

and

$$-\sigma_\rho{}^T + \sigma_\theta{}^T + 2i\sigma_{\rho\theta}{}^T = -\frac{2K\overline{\omega(\zeta)}}{\rho^2\overline{\omega'(\zeta)}}\left[2\zeta - \frac{\omega(\zeta)}{\omega'(\zeta)} - \frac{\zeta\omega(\zeta)\omega''(\zeta)}{[\omega'(\zeta)]^2}\right] + \frac{2\zeta}{\bar{\zeta}\,\overline{\omega'(\zeta)}}\left[\frac{\overline{\omega(\zeta)}\varphi''(\zeta)}{\omega''(\zeta)} - \frac{\overline{\omega(\zeta)}\varphi'(\zeta)\omega''(\zeta)}{[\omega'(\zeta)]^2} + \psi'(\zeta)\right] \tag{20}$$

where K is defined by Eq. (13), and the superscript T denotes total stresses. Similarly, the total displacements are obtained by combining the displacements from Eq. (9) with those resulting from the substitution of Eqs. (12) into Eq. (4). Some reduction gives

$$u_\rho{}^T + iu_\theta{}^T = \frac{\bar{\zeta}\,\overline{\omega'(\zeta)}}{\rho|\,\omega'(\zeta)|}\left[\frac{7-\varkappa}{4}\alpha U_0\omega(\zeta) - \frac{K(1+\varkappa)}{2\mu}\sum_{n=0}^{n=m}\frac{C_n\zeta^{1-np}}{1-np} + \frac{K}{2\mu}\frac{\omega(\zeta)\overline{\omega(\zeta)}}{\bar{\zeta}\,\overline{\omega'(\zeta)}} + \frac{K}{\mu}\omega(\zeta)\ln(\rho)\right] + \frac{\bar{\zeta}\,\overline{\omega'(\zeta)}}{2\mu\rho|\,\omega'(\zeta)|}\times\left[\varkappa\varphi(\zeta) - \frac{\omega(\zeta)\overline{\varphi'(\zeta)}}{\overline{\omega'(\zeta)}} - \overline{\psi(\zeta)}\right] \tag{21}$$

where superscript T denotes total displacement.

Two infinite systems of simultaneous equations can be obtained for the coefficients a_n and b_n in the series expansions of $\varphi(\zeta)$ and $\psi(\zeta)$ by expanding $\omega/\bar{\omega}'$ and the right sides of Eqs. (15) into power series, inserting the power series for $\varphi(\zeta)$ and $\psi(\zeta)$, and comparing coefficients of corresponding powers of σ. The necessary term by term multiplication of power series will be assumed permissible. The validity of $\varphi(\zeta)$ and $\psi(\zeta)$ determined in this manner can readily be checked by verifying that these functions yield the required boundary stresses.

Consider the expansion of $\omega/\bar{\omega}'$ into a power series on a contour $|\zeta| = \rho \ge 1$. It follows from the assumed conformality of the mapping and the form of Eq. (1) that the $\omega/\bar{\omega}'$ can be expanded as

$$\frac{\omega(\rho_j\sigma)}{\overline{\omega'(\rho_j\sigma)}} = \sum_{n=-m}^{n=\infty} K_n{}^{(j)}\sigma^{1+np} \qquad j = 0, 1 \tag{22}$$

Cross multiplication by $\overline{\omega'(\rho_j\sigma)}$ in the last equation and comparison of coefficients of corresponding powers of σ give a system of simultaneous equations for determination of $K_n{}^{(j)}$. This system is triangular, and the $K_n{}^{(j)}$ can be determined successively in the order $K_{-m}^{(j)}$, $K_{-m+1}^{(j)}$, ... It is found that

$$K_{-n}^{(j)} = \frac{1}{C_0}\left[C_n\rho_j{}^{1-np} - \sum_{t=1}^{t=m-n}(1-pt)C_t\rho_j{}^{-pt}K_{-n-t}^{(j)}\right] \qquad n = m, m-1, \ldots, 0 \tag{23}$$

For $n = m$, the summation terms on the right side of Eq. (23) are to be taken as zero. For positive orders, the $K_n{}^{(j)}$ are given by

$$K_n{}^{(j)} = -\frac{1}{C_0}\sum_{t=1}^{t=m}(1-pt)\rho_j{}^{-pt}C_tK_{n-t}^{(j)} \qquad n = 1, 2, \ldots \tag{24}$$

Similarly, the function $\omega\bar{\omega}/\bar{\zeta}\bar{\omega}'$ can be expanded in the form

$$\frac{\omega(\rho_j\sigma)\overline{\omega(\rho_j\sigma)}}{\rho_j\bar{\sigma}\,\overline{\omega'(\rho_j\sigma)}} = \sum_{n=-m}^{n=\infty} T_n{}^{(j)}\sigma^{1+np} \tag{25}$$

Substitution of Eqs. (1) and (22) into Eq. (25) then shows that

$$T_{-n}^{(j)} = \sum_{t=0}^{t=m-n} C_t\rho_j{}^{-pt}K_{-n-t}^{(j)} \qquad n = m, m-1, \ldots, 1, 0 \tag{26}$$

and

$$T_n{}^{(j)} = \sum_{t=0}^{t=m} C_t\rho_j{}^{-pt}K_{-n-t}^{(j)} \qquad n = 1, 2, \ldots \tag{27}$$

It follows from the preceding results that Eq. (15) can be represented in the general form

$$\varphi(\rho_j\sigma) + \frac{\omega(\rho_j\sigma)\,\varphi'(\rho_j\sigma)}{\overline{\omega'(\rho_j\sigma)}} + \overline{\psi(\rho_j\sigma)} = \sum_{n=-\infty}^{n=\infty} A_n^{(j)}\sigma^{1+np} \qquad j = 0, 1 \quad (28)$$

where, for the case considered here, the $A_n^{(j)}$ are zero for $n < -m$. When the series expansions of φ, ψ, and $\omega/\bar{\omega}'$ are substituted into the last relation, comparison of like powers of σ yields

$$a_n\rho_j^{1-np} + \sum_{t=-m}^{t=\infty} [1 + (n+t)p]K_t^{(j)}\,\rho_j^{p(t+n)}a_{-n-t} + b_{-n}\rho_j^{np-1} = A_{-n}^{(j)} \qquad j = 0, 1 \quad (29)$$

Furthermore, when the equation for $j = 1$ is multiplied by ρ_1^{1-np} and is subtracted from the equation for $j = 0$, the following infinite system of simultaneous equations results for determination of the coefficients a_n:

$$a_n(1 - b^{2-2np}) + \sum_{t=-m}^{t=\infty} [1 + (n+t)p] \times [K_t^{(1)} - K_t^{(2)}b^{1+p^t}]a_{-n-t} = A_{-n}^{(1)} - A_{-n}^{(2)}b^{1-np} \qquad -\infty < n < \infty \quad (30)$$

where use has been made of the fact that $\rho_0 = 1$ and $\rho_1 = b$.

In applied problems, it is often found that such a system of equations can be solved approximately by taking all the a_n to be zero except for n in some range $-n_0 \leq n \leq n_1$ where n_0 and n_1 are large integers. Solution of the truncated system of equations gives approximate values for $a_{-n_0}, \ldots, a_0, \ldots, a_{n_1}$. If the infinite system of Eqs. (30) has a solution, the accuracy of the approximate values computed for the a_n from the truncated system should improve with increasing n_0 and n_1 (see Chap. 1 of Ref. 8). The rate of improvement will, of course, depend on the rapidity of convergence of the function $\varphi(\zeta)$. It has been found for a case where $p = 4$, $m = 3$, and $b = 2.5244$ that such a system could be solved effectively without retaining a large number of terms.[11] The relative magnitudes of the matrix coefficients were such that the a_n for positive values of n were essentially independent of those for negative values of n. This made it possible to solve for the a_n without matrix inversion.

The effectiveness of the procedure employed in Ref. 11 depends on the rate of convergence of the mapping function and the magnitude of b. The convergence rate of $\varphi(\zeta)$ appears to increase with increasing b and decreasing m. In the problems of interest in this investigation, a mapping function of more than one hundred terms may be necessary to acquire the desired mapping accuracy. It seems likely that slow convergence of $\omega(\zeta)$ will also be accompanied by slow convergence of $\varphi(\zeta)$, and it may be necessary to consider truncated systems of prohibitively high order if reliable approximations are to be obtained for the coefficients a_n.

A different approach is presented below which permits precise satisfaction of the internal boundary condition while giving an approximate satisfaction of the external boundary condition with the accuracy of the approximation improving as b increases. This solution is based on consideration of an infinite plane having a star-shaped perforation. The plane is subjected to a uniform stress at infinity and a perforation boundary loading corresponding to Eq. (16) for $j = 0$. This problem is solved exactly, and the stress at infinity is adjusted so that, on the circle $|\zeta| = b$, Eq. (16) for $j = 1$ is satisfied except for small residual stress differences that decrease with increasing b.

In the analysis, it is assumed that b is large enough so that the following approximations are valid for $|\zeta| \geq b$:

$$\omega(\zeta) = C_0\zeta + C_1\zeta^{1-p} = C_0\rho\sigma + C_1\rho^{1-p}\sigma^{1-p} \quad (31)$$

$$\frac{1}{\omega(\zeta)} = \frac{1}{C_0}\zeta^{-1} - \frac{C_1}{C_0^2}\zeta^{-1-p} = \frac{1}{C_0}\rho^{-1}\sigma^{-1} - \frac{C_1}{C_0^2}\rho^{-p-1}\sigma^{-1-p} \quad (32)$$

$$\frac{1}{\omega'(\zeta)} = \frac{1}{C_0} + \frac{(p-1)C_1}{C_0^2}\rho^{-p}\sigma^{-p} \quad (33)$$

Then the boundary stresses corresponding to Eq. (16) for $j = 1$ are found to be

$$N_1 + iT_1 = 2K\ln(b) - P_1 + K + [Kp(p+1)C_1/C_0]b^{-p}\sigma^p \quad (34)$$

The stress functions for an infinite plane with a star-shaped perforation subjected to the assumed boundary stresses and a uniform tension S at infinity can be taken in the form

$$\varphi(\zeta) = a_0\zeta + \sum_{n=1}^{n=\infty} a_n\zeta^{1-np}, \qquad a_0 = \frac{SC_0}{2} \quad (35)$$

and

$$\psi(\zeta) = \sum_{n=0}^{n=\infty} b_n\zeta^{-1-np} \quad (36)$$

where the a_n and b_n are real. Substitution of Eqs. (22, 25, 35, and 36) into Eq. (15) for $j = 0$ followed by comparison of like powers of σ shows that

$$\left.\begin{aligned} a_n + Q_{-n} &= KT_n^{(0)} - a_0K_{-n}^{(0)} - P_0C_n && 1 \leq n \leq m-1 \\ a_m &= KT_{-m}^{(0)} - a_0K_{-m}^{(0)} - P_0C_m \\ a_n &= 0 && n \geq m+1 \end{aligned}\right\} \quad (37)$$

where

$$Q_n = \sum_{t=1}^{t=n+m} K_{n-t}^{(0)}(1 - pt)a_t \qquad n \geq 1 - m \quad (38)$$

The finite set of linear simultaneous equations (37) can be solved for the a_n, and determination of $\varphi(\zeta)$ is complete.

The function $\psi(\zeta)$ can be evaluated in terms of $\varphi(\zeta)$ by use of Eq. (15) for $j = 0$. Conjugation of this equation followed by a Cauchy integration around the unit circle shows that

$$\psi(\zeta) = \frac{1}{2\pi i}\oint_\gamma \frac{\overline{\varphi(\sigma)}\,d\sigma}{\sigma - \zeta} + \frac{1}{2\pi i}\oint_\gamma \frac{\overline{\omega(\sigma)}\,\varphi'(\sigma)\,d\sigma}{\omega'(\sigma)[\sigma - \zeta]} - K\frac{1}{2\pi i}\oint_\gamma \frac{\omega(\sigma)\overline{\omega(\sigma)}\,d\sigma}{\sigma\omega'(\sigma)[\sigma - \zeta]} + \frac{P_0}{2\pi i}\oint_\gamma \frac{\overline{\omega(\sigma)}\,d\sigma}{\sigma - \zeta} \quad (39)$$

and evaluation of these integrals yields

$$\psi(\zeta) = -\varphi\left(\frac{1}{\zeta}\right) - \frac{\omega(1/\zeta)\,\varphi'(\zeta)}{\omega'(\zeta)} + K\frac{\omega(\zeta)\omega(1/\zeta)}{\zeta\omega'(\zeta)} - P_0\omega\left(\frac{1}{\zeta}\right) \quad (40)$$

Alternately, $\psi(\zeta)$ can be expressed in series form as

$$\psi(\zeta) = (-a_0 - P_0C_0)\zeta^{-1} - \sum_{n=0}^{n=\infty}[a_0K_n^{(0)} + Q_n]\,\zeta^{-1-np} + K\sum_{n=0}^{n=\infty} T_n^{(0)}\zeta^{-1-np} \quad (41)$$

where the last equation follows from the series expansion of Eq. (15) for $j = 0$.

This completes the solution for the infinite plane with a star-shaped hole. Stresses and displacements can be computed from Eqs. (19-21). It now remains to adjust the stress value S at infinity so that the conditions on the external boundary of R are approximately satisfied. It will be

assumed that, for $\rho \geq b$, the following approximations are valid:

$$\omega(\zeta) = C_0\zeta + C_1\zeta^{1-p} \tag{42}$$

$$\varphi(\zeta) = a_0\zeta + a_1\zeta^{1-p} \tag{43}$$

$$\psi(\zeta) = b_0\zeta^{-1} + b_1\zeta^{-1-p} \tag{44}$$

It can be shown that, when terms of the order $|\zeta|^{1-2p}$ are neglected, the following asymptotic relations for total stresses and displacements are obtained from Eqs. (19–21):

$$N^T(\theta) = -K[1 + 2\ln(\rho)] + S + \frac{b_0\rho^{-2}}{C_0} + \rho^{-p}\cos(p\theta)\left[-\frac{Kp(1+p)C_1}{C_0} - \frac{S(1-p)(2+p)C_1}{2C_0} + \frac{(1-p)(2+p)a_1}{C_0} - \frac{(1-p)C_1b_0\rho^{-2}}{C_0^2} + \frac{(1+p)b_1\rho^{-2}}{C_0}\right] \tag{45}$$

$$T^T(\theta) = \rho^{-p}\sin(p\theta)\left[-\frac{Kp(1+p)C_1}{C_0} - \frac{Sp(1-p)C_1}{2C_0} + \frac{p(1-p)a_1}{C_0} + \frac{(1-p)C_1b_0\rho^{-2}}{C_0^2} + \frac{(1+p)b_1\rho^{-2}}{C_0}\right] \tag{46}$$

$$u_\rho{}^T = \left[\frac{(7-\kappa)\alpha U_0C_0\rho}{4} + \frac{K\rho C_0\ln(\rho)}{\mu} - \frac{\kappa KC_0\rho}{2\mu} + \frac{(\kappa-1)SC_0\rho}{4\mu} - \frac{b_0\rho^{-1}}{2\mu}\right] + \rho^{1-p}\cos(p\theta)\left[\frac{(7-\kappa)\alpha U_0C_1}{4} + \frac{KC_1\ln(\rho)}{\mu} - \frac{KC_1(\kappa+p^2)}{2\mu(1-p)} - \frac{pSC_1}{4\mu} + \frac{(\kappa-1+p)a_1}{2\mu} - \frac{b_1\rho^{-2}}{2\mu}\right] \tag{47}$$

$$u_\theta{}^T = \rho^{1-p}\sin(p\theta)\left[-\frac{p(7-\kappa)\alpha U_0C_1}{4} - \frac{pKC_1\ln(\rho)}{\mu} - \frac{p(1+\kappa)(p-2)KC_1}{2(1-p)\mu} + \frac{(1+\kappa-\kappa p)SC_1}{4\mu} - \frac{(\kappa+1-p)a_1}{2\mu} - \frac{(1-p)C_1b_0\rho^{-2}}{2\mu C_0} - \frac{b_1\rho^{-2}}{2\mu}\right] \tag{48}$$

The constants a_1, b_0, and b_1 depend linearly on K, S, and P_0. For $|\zeta| = b$, the required stress conditions should be $N^T(\theta) = -P_1$, $T^T(\theta) = 0$. It can be seen from Eqs. (45) and (46) that this is satisfied approximately by choosing S so that

$$S + (b_0b^{-2}/C_0) = -P_1 + K[1 + 2\ln(b)] \tag{49}$$

Then an exact solution is obtained for stresses in a doubly connected region having constant internal and external temperatures U_0 and U_1, respectively, and boundary stresses of the form

$$N_0 + iT_0 = -P_0 \qquad |\zeta| = 1 \tag{50}$$

and

$$N_1 + iT_1 = -P_1 + b^{-p}[A^*\cos p\theta + iB^*\sin p\theta] \qquad |\zeta| = b \tag{51}$$

When b is sufficiently large, the sinusoidal stress components in Eq. (51) become small, and the external stress is essentially uniform.

Analysis of Case-Bonded Grains

The preceding stress relations can be employed to deduce by superposition the effect of bonding the external boundary of the propellant grain to an elastic case.

When the stress S is chosen arbitrarily, a solution is obtained for stresses and displacements in a doubly connected region subjected to steady thermal gradients, a uniform internal pressure P_0, and external stresses and displacements closely approximated as

$$N + iT = A + B\cos(p\theta) + iC\sin(p\theta) \tag{52}$$

and

$$u_r + iu_\theta = D + E\cos(p\theta) + iF\sin(p\theta) \tag{53}$$

where the constants A through F depend linearly on P_0, K, and S. In the last two equations it is assumed that $|\zeta| = b$ maps essentially into a circle so that the external boundary stresses and displacements may be regarded as components referred to polar coordinates (r, θ). The coefficients of the sinusoidal terms are generally small in comparison to the constant terms, except when b is nearly equal to one.

If the sinusoidal terms in the last two equations are negligible in comparison with the constant terms, as often happens for practical grain configurations, it is possible to deduce the effect of case bonding. Let u_1 and k_1 denote, respectively, the values of A and D for P_0 and K arbitrarily fixed and for $S = 0$. Similarly, let u_2 and k_2 denote the corresponding quantities for $P_0 = K = 0$ and $S = 1$. Then superposition gives for the external boundary of the propellant grain

$$u_r = u_1 + u_2S \qquad N = k_1 + k_2S \tag{54}$$

Now let a circular ring that is in plane strain with internal and external radii R_1 and R_1, respectively, be subjected to an internal radial stress N and a temperature change U_1. The resulting internal displacement[1] is

$$u_r = \frac{(2\delta + \kappa_c - 1)R_1N}{4(\delta-1)\mu_c} + (1+\nu_c)\alpha_cU_1 = -A_cN + (1+\nu_c)\alpha_cU_1 \tag{55}$$

where $\delta = R_2^2/R_1^2$, μ_c and κ_c are elastic constants of the ring, and α_c is the coefficient of thermal expansion. Then it is found from Eqs. (54) and (55) that, in order for the displacements on the external boundary of the grain to match with the internal displacements in the case, the stress at infinity must be given by

$$S = \frac{(1+\nu_c)\alpha_cU_1 - u_1 - k_1A_c}{u_2 + k_2A_c} \tag{56}$$

This stress at infinity simulates the effect of a case. Stresses and displacements for the case-bonded grain can then be computed from Eqs. (19–21) with $1 \leq |\zeta| \leq b$.

If the sinusoidal terms in Eqs. (52) and (53) are not negligible, then the superposition procedure must be modified. Let a circular ring be loaded by an internal stress distribution of the form given by Eq. (52). The resulting internal boundary displacements are of the form

$$u_r + iu_\theta = D_c + E_c\cos(p\theta) + iF_c\sin(p\theta) \tag{57}$$

where D_c, E_c, and F_c depend on A, B, C, R_1, R_2 and the ring elastic properties. Explicit expressions for D_c, E_c, and F_c, along with special approximate forms valid for small ring thickness, are obtained in Ref. 1.

Let the constants P_0, K, S and the propellant elastic properties be fixed so that all parameters in Eqs. (52) and (53) are determined, and consider the problem of regulating the thickness and elastic properties of the ring such that the ring and propellant grain displacements correspond closely. If the propellant and ring displacements are required to coincide for $\theta = 0$ and $\theta = \pi/p$, it follows from Eqs. (53) and (57) that

$$D = D_c \qquad E = E_c \tag{58}$$

If these two relations are satisfied, then the case and propellant displacements will agree exactly, except for the differ-

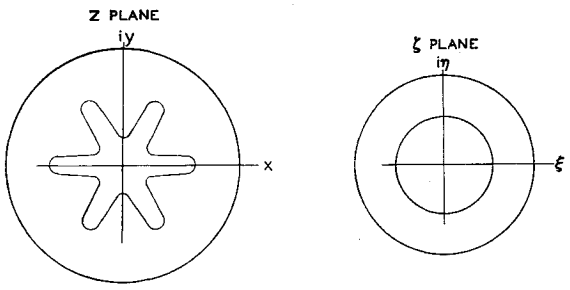

Fig. 1 Mapping correspondence for a solid propellant grain.

ences of the tangential displacement components which are usually small compared to the normal components. When Poisson's ratio for the case is selected, Eqs. (58) can be solved simultaneously for the case thickness and elastic modulus. Various combinations of case properties can be computed by choosing different values of S. Although this method has the disadvantage of not permitting independent specification of all case properties, it was shown in Ref. 7 that, for an internally pressurized grain with four star points, realistic combinations of case parameters could be computed in this manner. Assuming that practical combinations of case properties can be obtained, a further check on the validity of the superposition procedure should be made to ascertain that the computed differences of circumferential displacements in the case and the propellant grain are negligible.

Numerical Computations

A digital computer program based on the preceding analysis was written to determine stresses in a propellant grain subjected to steady thermal gradients, internal pressure, and either external pressure or case bonding.‡ The program input parameters are the coefficients C_n in Eq. (1) which define the internal geometry, the outer radius of the grain, the physical properties of the propellant, the boundary temperatures and pressures, and the case thickness and physical properties if a bonded grain is considered. The case superposition was made under the assumption that Eq. (56) is valid. The uniform propellant shrinkage problem can be treated as a special thermal stress problem by taking $U_0 = U_1$ with the product of the thermal expansion coefficient of the grain and the grain temperature equal to the negative of the unit strain due to shrinkage. The grain must, of course, be case bonded in order for shrinkage stresses to result.

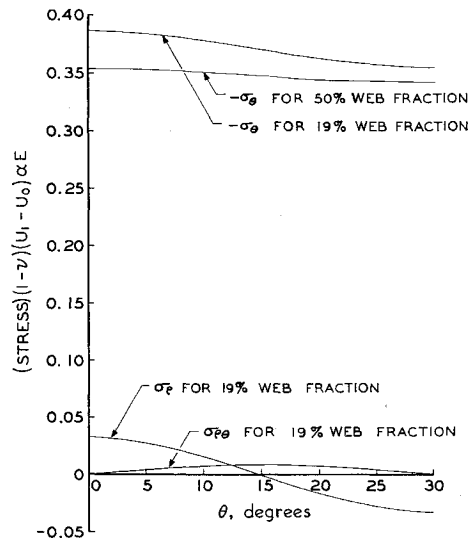

Fig. 2 Stresses on the external boundary of a thermally stressed propellant grain.

‡ The necessary programs were written by C. C. Fretwell, Department of Theoretical and Applied Mechanics, University of Illinois.

In the approximate solution of the propellant grain stress problem for a doubly connected region by consideration of a related problem for an infinite plate with a perforation, the accuracy of the approximation improves with increasing web fraction. The two factors of primary importance in testing the validity of the approximations are, first, how nearly the curve $|\zeta| = b$ maps into a circle and, second, how closely the external boundary stresses given by Eq. (16) for $j = 1$ and the stresses on a related contour in the infinite solid coincide. To examine these factors, example computations are presented below for thermal stresses in an unpressurized, unbonded grain with the internal geometry from Fig. 1 and web fractions of 50 and 19%.

A fifty-term mapping series yielded a very accurate map except for some rounding of the inverse star points not existing in the actual geometry. However, it is shown in Refs. 1 and 2 that this rounding can be reduced by increasing the number of terms in the mapping function.

It is evident from Eq. (37) that $\varphi(\zeta)$ is a finite polynomial of $m + 1$ terms. The function $\psi(\zeta)$ can be expressed as a rational function by Eq. (40) or as an infinite series by Eq. (41). Although the rational function expression for $\psi(\zeta)$ is exact, it is not well suited for numerical computations unless $|\zeta| = 1$, because $\omega(\zeta^{-1})$ and $\varphi(\zeta^{-1})$ may be complex numbers of very large absolute value when $|\zeta| > 1$. For this reason, Eq. (41) was employed. The series for $\psi(\zeta)$ was truncated after one hundred terms. This approximation resulted in small normal stresses at the internal boundary. However, the magnitude of these stresses was only about 0.5% of the corresponding circumferential stresses. This error was considered negligible, but it could have been further reduced by increasing the number of terms retained in the series for $\psi(\zeta)$.

It was shown previously that, for the geometrical configuration in Fig. 1, the deviation of the external boundary from a circle is insignificant at least down to web fractions of 19%. The stresses computed for $|\zeta| = b$ agreed closely with the form indicated by Eq. (52). The dependence of A, B, and C on the parameters K and S is indicated in Table 1. The relative magnitudes of the constant and sinusoidal terms are also shown. The pressure P_0 does not enter, since it was taken equal to zero. The value of S necessary to cancel the uniform component of external normal stress is evidently equal to $-A_k/A_s$, where A_k denotes the value of A for $K = 1$ and $S = 0$, and A_s denotes the value of A for $K = 0$ and $S = 1$. There then remain certain residual sinusoidally varying normal and shear stresses on the external boundary.

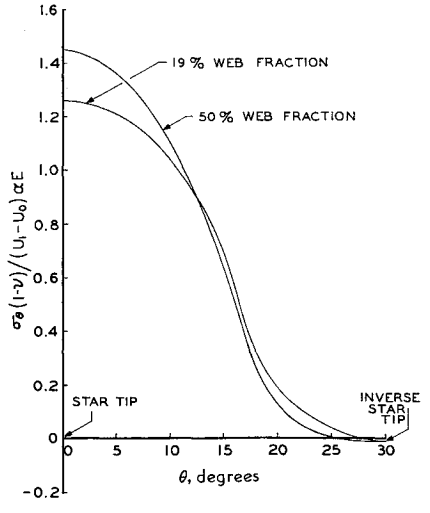

Fig. 3 Circumferential stresses on the internal boundary of a thermally stressed propellant grain.

Table 1 External boundary stresses

Web fraction	K	S	A	B	C	B/A	C/A
0.19	1	0	−1.8570	−0.2058	−0.2049	0.111	0.110
0.19	0	1	0.6693	0.1032	0.0826	0.154	0.124
0.50	1	0	−2.4240	−0.0650	−0.0628	0.027	0.026
0.50	0	1	0.7846	0.0325	0.0252	0.041	0.032

The residual stresses, as well as the circumferential stresses at the external boundary, are shown in Fig. 2. For a 50% web fraction, the magnitudes of the residual normal and shearing stresses were found to be everywhere less than 3% of the corresponding circumferential stresses and are not included in the figure. These residual stresses should give only a small error in circumferential stresses computed at the outer boundary and a completely negligible effect at the internal boundary where accurate stress determination is most important.

For a 19% web fraction, the residual external boundary stresses were not small. It can be seen from Fig. 2 that in this instance the magnitudes of the σ_ρ and $\sigma_{\rho\theta}$ components were as large as 9% of the corresponding σ_θ components. These residual stresses certainly do not have a negligible effect at the external boundary. However, it may still be possible that they have only a slight effect on the stresses at the internal boundary.

It is interesting to compare the circumferential stresses in Fig. 2 with corresponding stresses in hollow cylinders of the same web fraction. By use of the hollow cylinder thermal-stress solution given in Ref. 10, it is found that the ratios of the external circumferential stress in the propellant grain to the external circumferential stress in the cylinder are equal to 0.895 and 0.792 for web fractions of 50 and 19%, respectively.

Figure 3 shows the circumferential stress distribution at the internal boundary of the propellant grain caused by thermal gradients, zero internal pressure, and the residual external normal and shear stresses. As was expected, the internal boundary stresses are greatest near the star tip and become almost zero at the inverse star tip.

Table 1 can be employed in solving a problem for a propellant grain subjected only to uniform external pressure. This corresponds to the instance where $K = P_0 = 0$, and S must be chosen to simulate the desired external boundary stress. It can be seen from Table 1 that the external boundary stresses will not actually be uniform because of the presence of the sinusoidal terms involving the constants B and C, and these terms will cause some error in the stresses computed at the internal boundary of the grain. A rough estimate of the magnitude of the error can be obtained by considering the error in the internal boundary stress for a hollow circular cylinder of the same web fraction. For cylinders with 19 and 50% web fractions, the respective ratios of thickness to internal radius are 0.235 and 0.5. If, instead of a uniform external pressure, these cylinders are subjected to external stresses according to the second and fourth entries in Table 1, the corresponding errors in maximum circumferential stresses at the internal boundary are found from elementary stress relations for a circular ring to be 12.1 and 1.2% for web fractions of 19 and 50%, respectively.

Conclusion

A practical theoretical method has been presented for determining stresses and displacements in star-perforated solid-propellant grains caused by pressurization, steady thermal gradients, and shrinkage. The only limitations on the method are that the geometry must be describable by a mapping series with a reasonable number of terms and that the web fraction must be sufficiently large so that the approximations made concerning external boundary stresses are valid. In the instance where the web fraction is small, the problem still can be treated by solving the infinite system of Eqs. (30). It might then be more efficient to follow a completely different approach whereby the internal boundary conditions are satisfied identically and the external boundary conditions are satisfied pointwise as indicated in Ref. 12. Yet another method of solution could be based on representing the two complex stress functions in terms of Cauchy integrals containing a single unknown density function governed by a certain integral equation (see article 102 of Ref. 9). However, solving the integral equation and evaluating the stresses and displacements would be difficult.

The author believes that the theoretical method presented here possesses advantages over experimental methods since the required computations are no more expensive, and the theoretical method can readily be extended to account for viscoelastic effects. Furthermore, the analytical method is faster once a general computer program has been written.

In closing, mention will be made of a related propellant grain stress problem that is also of considerable practical importance. This is the problem of determining stresses due to transverse acceleration loading in case-bonded grains. In Ref. 1, a formulation of this problem is given for the instance of a rigid case. The analysis is reduced to consideration of infinite systems of simultaneous equations that can be treated by approximate methods.

References

[1] Wilson, H. B., Jr. and Fretwell, C. C., "A method of conformal mapping and the determination of stresses in solid-propellant rocket grains," Rohm & Haas Co., Rept. S-38 (April 1963); also Armed Services Technical Information Agency AD-299979.

[2] Wilson, H. B., Jr. and Becker, E. B., "An effective numerical method for conformal mapping of simply connected regions," Intern. J. Eng. Sci. (submitted for publication).

[3] Cost, T. L., "Approximate Laplace transform inversion techniques in viscoelastic stress analysis," Rohm & Haas Co., Rept. P-63-13 (July 1963).

[4] Ordahl, D. D. and Williams, M. L., "Preliminary photoelastic design data for stresses in rocket grains," Jet Propulsion **27**, 657–662 (1957).

[5] Durelli, A. J., "Photothermoelastic analysis of bonded propellant grains," Exptl. Mech. **1**, 97–104 (1961).

[6] Fourney, M. E. and Parmeter, R. R., "Stress concentration data for internally perforated grains," Bureau of Naval Weapons Rept. 7758, Naval Ordnance Test Station TP 2728 (December 1961).

[7] Wilson, H. B., Jr., "Stresses owing to internal pressure in solid propellant rocket grains," ARS J. **31**, 309–317 (1961).

[8] Kantorovich, L. V. and Krylov, V. I., *Approximate Methods of Higher Analysis* (Interscience Publishers Inc., New York, 1953), 3rd ed.

[9] Muskhelishvili, N. I., *Some Basic Problems of the Mathematical Theory of Elasticity* (P. Noordhoff Ltd., Groningen, Holland, 1953).

[10] Timoshenko, S. and Goodier, J. N., *Theory of Elasticity* (McGraw-Hill Book Co., Inc., New York, 1951), 2nd ed., pp. 399–437.

[11] Sutherland, R. D., Manville, S. M., Schneider, K. J., Shook, R. G., and White, F. M., Jr., "Thermal stresses in perforated plates and bodies of revolution," General Dynamics Corp., Rept. TM-349-35 (June 1961).

[12] Davies, G. A. O., "Stresses around a reinforced circular hole near a reinforced straight edge," Aeronaut. Quart. **14**, 374–386 (November 1963).